Infectious Disease Modelling 8 (2023) 632–644

Contents lists available at ScienceDirect

Infectious Disease Modelling

journal homepage: www.keaipublishing.com/idm

The dynamics of the risk perception on a social network and its effect on disease dynamics

Meili Li [a], Yuhan Ling [a], Junling Ma [b, *]

[a] College of Science, Donghua University, Shanghai, 201620, China
[b] Department of Mathematics and Statistics, University of Victoria, Victoria, BC, V8W 2Y2, Canada

ARTICLE INFO

Article history:
Received 22 March 2023
Received in revised form 12 May 2023
Accepted 28 May 2023
Available online 7 June 2023
Handling Editor: Dr Yijun Lou

Keywords:
Risk perception
Social network
Contact network
Information dynamics

ABSTRACT

The perceived infection risk changes individual behaviors, which further affects the disease dynamics. This perception is influenced by social communication, including surveying their social network neighbors about the fraction of infected neighbors and averaging their neighbors' perception of the risk. We model the interaction of disease dynamics and risk perception on a two-layer random network that combines a social network layer with a contact network layer. We found that if information spreads much faster than disease, then all individuals converge on the true prevalence of the disease. On the other hand, if the two dynamics have comparable speeds, the risk perception still converges to a value uniformly on the network. However, the perception lags behind the true prevalence and has a lower peak value. We also study the behavior change caused by the perception of infection risk. This behavior change may affect the disease dynamics by reducing the transmission rate along the edges of the contact network or by breaking edges and isolating the infectious individuals. The effects on the basic reproduction number, the peak size, and the final size are studied. We found that these two effects give the same basic reproduction number. We find edge-breaking has a larger effect on reducing the final size, while reducing the transmission rate has a larger effect on reducing the peak size, which is true for both scale-free and Poisson networks.

1. Introduction

Individuals may change their behavior during an epidemic in response to their perception of disease infection risks (Ferguson, 2007). This phenomenon has been observed in many disease outbreaks, including the behavior change during the historical plague outbreaks (Riva et al., 2014), the HIV epidemic (Akwara et al., 2003; Howard, 2006), and the recent COVID-19 pandemic (Magnan et al., 2021; Savadori & Lauriola, 2022). These behavior changes affect the dynamics of the disease outbreak.

There has been a large body of research on modeling behavior change and disease outbreaks. However, most of these researchers assume that the awareness of disease infection risk is related to the precise disease prevalence information.

* Corresponding author.
E-mail address: junlingm@uvic.ca (J. Ma).
Peer review under responsibility of KeAi Communications Co., Ltd.

https://doi.org/10.1016/j.idm.2023.05.006

Bagnoli et al. (2007) investigated the effects of risk perception in a simple model of epidemic spreading. They assumed that the perception of the infection risk depends on the fraction of ill neighbors. Likewise, Wang et al. (2009) assumed that the perception of the risk of being infected relies on the fraction of infected neighbors. Li et al. (2020) considered two kinds of awareness: the local one represented by the fraction of infectious neighbors, and the global one represented by the prevalence of the disease in the population.

The assumption that the awareness of disease infection risk depends on the precise information about disease prevalence maybe realistic when extensive surveillance for the prevalence has been given. However, during the beginning of an outbreak, such information is generally unavailable or not precise. During such an initial phase of an epidemic, individuals rely on social communication to obtain such information. Also, existing research has found that most available information comes not from physical contact or mainstream media but from social networks (Chew & Eysenbach, 2010; Ginsberg et al., 2008). Information's spread speed is increasing with the development of science and technology. People can quickly assess and communicate the situation of infectious diseases (Stieglitz & Linh, 2013). Therefore, studying the information we get from social networks is increasingly important.

There is a large body of research on the diffusion of information on the social network, including both small networks and large random networks. For a small network, a finite-dimensional adjacency matrix generally represents the relationship between different nodes (Gomez et al., 2013; Granell et al., 2013; Xiao et al., 2019). For a large network which adjacency matrix is not readily available, a random network is usually used, which network connections are usually expressed by probability (Gallos et al., 2008; Ball et al., 2010).

A common research focus for information dissemination is about the spread of rumors, knowledge, and word of mouth, which are usually represented by discrete states for the nodes. For instance, Zhao et al. (2012) extended the classical Susceptible-Infected-Removed (SIR) rumor spreading model by introducing a new type of individual called “Hibernators”, which led to the establishment of the SIHR model. The researchers discussed the spreading threshold and established a relationship between the final size of the rumor and two probabilities. Furthermore, they found that the direct link from ignorants to stiflers advanced the rumor terminal time and reduced the maximum rumor influence. Wang et al. (2014) expanded the SIR model by introducing latent nodes to represent offline users who can receive but not spread information. This led to the development of the SEIR model. Based on the SEIR model, the researchers explained the information transmission mechanism of Social Networking Services (SNS) and established a dynamic model for SNS information transmission. The study of continuous information transmission is similar to the study of material flow because mass change is typically continuous. For example, Zhang and Padrino (2017) investigated purely diffusive transport in network systems and derived a mass balance equation. They calculated the closures for the ensemble-averaged mass transport equation by considering one-dimensional diffusion in the channels. Other scholars have studied the effects of network structure or certain parameters on information transmission. For example, Han et al. (2014) analyzed the mechanisms of rumor propagation and the topological properties of large-scale social networks. They proposed a novel model based on physical theory and found that rumor propagation is greatly influenced by various factors, including a rumor's attraction, the initial rumormonger, and the sending probability. Zhang et al. (2021) established a network public opinion diffusion model and confirmed that the scale of the network influences the time it takes to reach its peak. Additionally, they found that the number and degree of initial infection were negatively correlated with the size of the final infection.

The communication of disease infection risk on a social network is a particular type of the diffusion of information on a network, which has been extensively studied. Ferguson (2007) demonstrated that when people are aware of the outbreak of infectious diseases, they sometimes change their behavior to reduce the risk of infection, and this human response will significantly impact the spread of diseases. In 2009, Funk et al. (2009) studied the spread of awareness and its impact on the epidemic outbreak. They proved that the spread of awareness not only reduced the incidence of disease but also prevented the large-scale outbreak of the epidemic in some cases. Many scholars have combined research on information transmission with infectious disease transmission. For example, Peng et al. (2022) investigated a model for the competition between disease and awareness processes in a homogeneous network with natural birth and death processes. They found that the model dynamics were distinguished from simple SIS dynamics by a threshold value of the population birth rate. This threshold produced intriguing competing dynamics between awareness and epidemic spreading. There has been a lot of research on multi-layer networks as well. For instance, Massaro and Bagnoli (2014) developed a two-layer network to examine the interaction between epidemic transmission and risk perception in the UAU-SIR model. One layer represents the information networks, while the other represents the physical networks. Their research showed that the possibility of stopping an infection for a high precaution level is determined by the similarity between the physical and information networks. If the networks are too dissimilar, it is impossible to prevent epidemics. Granell et al. (2013) used a microscopic Markov chain approach to reveal the phase diagram of epidemics incidence and captured the evolution of the epidemic threshold depending on the topological structure of the multiplex and its interrelation with the awareness process. Interestingly, the critical point for an epidemic is defined by the awareness dynamics and the topology of the virtual network.

In this paper, we combine the dynamics of information spread on a random social network with the dynamics of disease spread on a contact network and study the effect of disease awareness on disease spread.

In Section 2, we establish a two-layer network, setting an infection risk perception model, and discuss two cases according to the speed of information spread. In Section 3, we consider the impact of risk perception on disease, mainly considering the impact on the basic reproduction number R_0, peak size, and final size. Conclusions are given in Section 4.

2. The interaction of information spread and disease dynamics

In this section, we study the dynamics of perceived disease infection risk on a two-layer random network. The first layer is a social network on which individuals communicate and evaluate disease infection risk, and the second layer is a contact network on which the disease spreads. Each node has two types of edges, namely the social network contacts and the contact network contacts. For each type, the edges form a network according to the configuration model. Specifically, for each node and each network type, a random degree is drawn from a degree distribution, and the same number of stubs (half-edges) are attached to the nodes. Two randomly selected stubs of the same type are connected to form an edge. Such edge forming procedure is repeated until no new edges can be formed. Self-loops, multiple edges and remaining stubs (if any) are dropped. Clustering and degree correlation of the configuration network are negligible (Rizzo et al., 2014). For simplicity, we assume that the degrees of the two networks are independent of each other.

We assume that individuals update their perception of the disease infection risk via contacts on the social network. Individuals communicate with their neighbors and take an average of their neighbors' perception risk, and then update their perception proportional to the difference between this average and their own perception. In addition, they survey the fraction of infectious neighbors on the social network, and update their perception proportional to the difference between this fraction and their own perception.

Because the degree distribution is the only characterizing statistics of the network, we classify the nodes by their degree on the social network. Lets K be the maximum degree of the social network, and $L = \sum_{k=1}^{K} kN_k$ be the total number of stubs, where N_k represents the number of nodes with degree k. Each individual (node) on the social network has a perception of the risk of disease infection. Let ρ_k be the perceived risk of infection by nodes with degree k.

Let ν be the information spread rate on the social network. For a degree-k node on the social network, the average perception of its neighbors is $\sum_{q=1}^{K} p_{q|k}\rho_q$, where $p_{q|k}$ is the probability that a neighbor of the degree-k node has a degree q on the social network. The infected proportion of its neighbors is $\sum_{q=1}^{K} p_{q|k}J_q$, where J_q is the proportion of infected with a degree q on the social network. Thus, the model construction in this section is as follows:

$$\dot{\rho_k} = \nu\Big(\underbrace{-\rho_k + \sum_{q=1}^{K} p_{q|k}\rho_q}_{\text{update from average neighbors' perception}} \underbrace{-\rho_k + \sum_{q=1}^{K} p_{q|k}J_q}_{\text{update from infected neighbors}}\Big).$$

For simplicity, here, we re-scale time so that $\nu = 1$. In Section 2.2, we will discuss the situation of ν more specifically. Thus, the above equation can be simplified as

$$\dot{\rho_k} = -\rho_k + \sum_{q=1}^{K} p_{q|k}\rho_q - \rho_k + \sum_{q=1}^{K} p_{q|k}J_q. \tag{1}$$

Because a configuration network has negligible degree correlation, we get

$$p_{q|k} = \frac{qN_q}{L}. \tag{2}$$

The evolution of infectious disease should be considered on the contact network, so we use a joint degree distribution $f(k_c, q)$, which is the probability that a random node has a degree k_c on the contact network and a degree q on the social network. Thus, the conditional probability $f(k_c|q)$ that a random node with a degree q on the social network has a degree k_c on the contact network can be calculated as

$$f(k_c|q) = \frac{f(k_c, q)}{p_q} = \frac{f(k_c, q)}{\sum_{k_c} f(k_c, q)}, \tag{3}$$

where p_q represents the degree distribution of the social network.

To calculate the probability J_q, note that a node has a degree k_c on the contact network and q on the social network is infectious with probability I_{k_c}. Thus,

$$J_q = E_{k_c}[J_q|k_c] = \sum_{k_c} I_{k_c} f(k_c|q),$$

where E_{k_c} means taking the mean of k_c. We assumed that the degrees on the social network and the contact network are independent, i.e.,

$$f(k_c, q) = \pi_{k_c} p_q, \text{ and thus } f(k_c|q) = \pi_{k_c},$$

where π_{k_c} represents the degree distribution of the contact network. Thus,

$$J_q = \sum_{k_c} I_{k_c} \pi_{k_c} = I. \tag{4}$$

Substituting (4) into (1), and combining with (2), we get

$$\begin{aligned}
\dot{\rho_k} &= -\rho_k + \sum_{q=1}^{K} p_{q|k}\rho_q - \rho_k + \sum_{q=1}^{K} p_{q|k} J_q \\
&= -2\rho_k + \sum_{q=1}^{K} p_{q|k}\rho_q + \sum_{q=1}^{K} p_{q|k} J_q \\
&= -2\rho_k + \frac{1}{L}\sum_{q=1}^{K} q N_q \rho_q + \sum_{q=1}^{K} I p_{q|k} \\
&= -2\rho_k + \frac{1}{L}\sum_{q=1}^{K} q N_q \rho_q + I, \quad k = 1, 2, \ldots, K.
\end{aligned}$$

This model can be rewritten in a matrix form:

$$\dot{\vec{x}} = -2\vec{x} + \frac{1}{L} N\vec{x} + I \cdot \vec{1} = \left(-2E + \frac{1}{L} N \right)\vec{x} + I \cdot \vec{1}, \tag{5}$$

where

$$\vec{x} = (\rho_1, \rho_2 \cdots, \rho_K)^T, \quad \vec{1} = (1, 1, \ldots, 1)^T, \tag{6}$$

$$N = \begin{pmatrix} N_1 & 2N_2 & \cdots & KN_K \\ N_1 & 2N_2 & \cdots & KN_K \\ \vdots & \vdots & \ddots & \vdots \\ N_1 & 2N_2 & \cdots & KN_K \end{pmatrix}, \tag{7}$$

and E is the unit matrix. Let

$$M = -2E + \frac{1}{L} N, \tag{8}$$

then (5) becomes

$$\dot{\vec{x}} = M\vec{x} + I\vec{1}. \tag{9}$$

To study the interaction between the information dynamics and disease dynamics, we consider the following two cases. The first is when information spreads much faster than disease spreads, and the second is when the two spread have comparable speed.

2.1. Information spreads much faster than disease

When information spreads much faster than disease spreads, $I(t)$ can be viewed as a constant relative to $\rho_k(t)$. The matrix N has a rank 1, and thus -1 is an eigenvalues of M with an associated eigenvector $\vec{1}$, while the other eigenvalues of M are all -2. Thus,

$$\vec{x}(\infty) = I\vec{1}.$$

That is, eventually every node has the same risk perception I, the true prevalence.

2.2. Disease and information dynamics have comparable speed

When the spread of disease and the spread of information have comparable speed, we need to consider the information transmission speed v on the social network. Like the derivation of equation (9), we can derive the following equation

$$\dot{\vec{x}} = v(M\vec{x} + I(t)\vec{1}). \tag{10}$$

Since the largest eigenvalue of M is -1 with the associated eigenvector $\vec{1}$ and the others are all -2, the solutions of (10) decay faster along the eigenspace corresponding to the eigenvalue -2. Thus, eventually solutions approach the eigenspace corresponding to the eigenvalue -1. For simplicity, we only consider the dynamics in the eigenspace, i.e., $\rho_1(t) = \rho_2(t) = \cdots = \rho_K(t) = \rho(t)$, that is, $\vec{x} = \rho \cdot \vec{1}$. Then (10) becomes

$$\dot{\rho}\vec{1} = v(M\rho\vec{1} + I\vec{1}) = v(-\rho + I)\vec{1}.$$

Thus, (10) is simplified to

$$\dot{\rho} = v(-\rho + I). \tag{11}$$

We now couple (11) with the disease model on the contact network by extending the following Miller-Volz (Volz, 2008; Miller, 2011) SIR epidemic model

$$\dot{\theta} = -\lambda\varphi, \tag{12}$$

$$\dot{\varphi} = \left[-\lambda - \gamma + \lambda\frac{g''(\theta)}{g'(1)}\right]\varphi, \tag{13}$$

$$\dot{I} = \lambda\varphi g'(\theta) - \gamma I, \tag{14}$$

$$S = g(\theta) = \sum_{k_c}\pi_{k_c}\theta^{k_c}, \tag{15}$$

where λ is the disease transmission rate along a random edge, and γ is the recovery rate of an infected node. $\theta(t)$ is the probability that a random neighbor of a susceptible node has not transmitted disease by time t. A degree-k_c node is susceptible if none of its neighbors have transmitted the infection. This occurs with a probability of θ^{k_c}. $\varphi(t)$ is the probability that

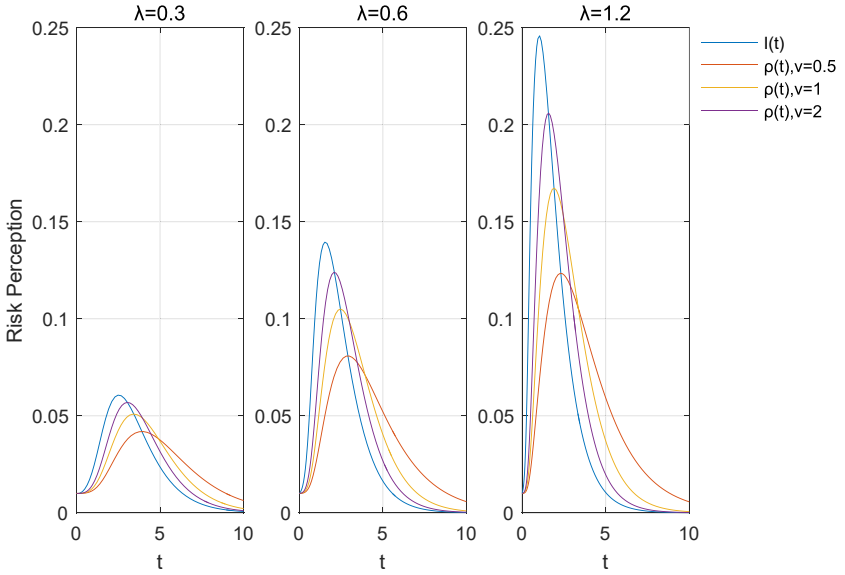

Fig. 1. The blue curves show the dynamics of the proportion of infected individuals $I(t)$, and the other curves are the risk perception $\rho(t)$, corresponding to the information transmission speed $v = 0.5, 1, 2$, respectively. The network is a scale-free network with a degree distribution $p_k \propto k^{-2}$ for $k = 1, 2, \cdots, 60$. We consider three infection rates, $\lambda = 0.3, 0.6, 1.2$. The recovery rate $\gamma = 1$. The initial conditions are $\theta_0 = 1$, $\varphi_0 = I_0 = \rho(0) = 0.01$.

an edge has not transmitted infection (θ edges) but can cause infection (i.e., connected to an infectious node). $g(\theta)$ is the probability generating function of the degree distribution π_{k_c}, so the fraction of nodes that are susceptible is $S = g(\theta)$.

Our aim is to study the behaviour change caused by the perception of infection risk, and the influence of information transmission speed v and infection rate λ on the dynamics of disease. We give the disease curves and risk perception curves by numerical simulation and show the results on scale-free network and Poisson network respectively. The result of scale-free network is shown in Fig. 1, in each little picture, the blue curve represents the dynamics of the proportion of infected persons $I(t)$, and the other three curves are the dynamics of risk perception $\rho(t)$, corresponding to different information transformation speed $v = 0.5, 1, 2$. Fig. 1 shows that the dynamics of risk perception lags behind the prevalence $I(t)$. In addition, the peak of risk perception is lower than the peak of the prevalence. As the infection rate increases, the gap between the peaks increases. The faster information spreads, the closer the risk perception is to the prevalence itself. The qualitative results on a Poisson network are the same, which is not shown here.

3. The effect of infection risk perception on disease dynamics

In this section we consider the impact of perception of infection risk on the disease dynamics. We consider two networks: the scale-free network and Poisson network. We consider two kinds of awareness: the initial awareness, and the awareness arised after the disease has begun to spread in the study area. We denote the initial reduction factor of awareness by e^{-b}, and the reduction factor of infection risk perception by $e^{-\alpha\rho}$, where b and α are the corresponding reduction coefficients of awareness. Let's first consider the models proposed by Li et al. (2020), which use the prevalence I as disease awareness. This model considers the effects of awareness on disease transmission in the following two cases:

Case 1 in Li et al. (2020) Awareness reduces infection rates. The corresponding model is

$$\dot{\theta} = -\lambda e^{-b-\alpha I}\varphi, \tag{16}$$

$$\dot{\varphi} = \lambda e^{-b-\alpha I}\left(\frac{g''(\theta)}{g'(1)} - 1\right)\varphi - \gamma\varphi, \tag{17}$$

$$\dot{I} = \lambda e^{-b-\alpha I}\varphi g'(\theta) - \gamma I. \tag{18}$$

Case 2 in Li et al. (2020) Awareness breaks infectious edges. The corresponding model is

$$\dot{\varphi} = \lambda\left(\frac{g''(\theta)}{g'(1)} - 1\right)\varphi - \gamma e^{b+\alpha I}\varphi, \tag{19}$$

$$\dot{\theta} = -\lambda\varphi, \tag{20}$$

$$\dot{I} = \lambda\varphi g'(\theta) - \gamma I. \tag{21}$$

Similarly, we also consider these two effects of awareness on disease transmission, but our models use the risk perception ρ as disease awareness. The specific models are as follows.

Case 1. Awareness leads to a decrease in infection rates. We assume that the infection rate is $\lambda e^{-b-\alpha\rho}$. Like Li et al. (2020), we substitute this infection rate into the Miller-Volz model (Volz, 2008; Miller, 2011), then we get.

$$\dot{\theta} = -\lambda e^{-b-\alpha\rho}\varphi, \tag{22}$$

$$\dot{\varphi} = \lambda e^{-b-\alpha\rho}\left(\frac{g''(\theta)}{g'(1)} - 1\right)\varphi - \gamma\varphi, \tag{23}$$

$$\dot{I} = \lambda e^{-b-\alpha\rho}\varphi g'(\theta) - \gamma I. \tag{24}$$

Case 2. Awareness breaks infectious edges. Like Li et al. (2020), the change of φ edge can be written as.

$$\dot{\varphi} = \lambda\left(\frac{g''(\theta)}{g'(1)} - 1\right)\varphi - \gamma e^{b+\alpha\rho}\varphi, \tag{25}$$

the other equations are the same, i.e.,

$$\dot{\theta} = -\lambda\varphi, \tag{26}$$

$$\dot{I} = \lambda\varphi g'(\theta) - \gamma I. \tag{27}$$

In the following subsections, we will examine the effects of awareness on the basic reproduction number, peak size and final epidemic size in these two cases.

3.1. The basic reproduction number

We use the next generation matrix method (Dreessche & Watmough, 2002) to compute the basic reproduction number R_0. As for awareness leads to a decrease in infection rates, note that the dynamics of I is determined by φ, so we only need to study equation (23) at the disease-free equilibrium ($\varphi = 0$, $I = 0$, $\rho = 0$, $\theta = 1$), that is

$$\dot{\varphi} = \lambda e^{-b}\left(\frac{g''(1)}{g'(1)} - 1\right)\varphi - \gamma\varphi = -(\lambda e^{-b} + \gamma)\varphi + \lambda e^{-b}\frac{g''(1)}{g'(1)}\varphi. \tag{28}$$

The new infection matrix is

$$F = \lambda e^{-b}\frac{g''(1)}{g'(1)}, \tag{29}$$

and the transition matrix is

$$V = \lambda e^{-b} + \gamma. \tag{30}$$

Thus

$$R_0 = FV^{-1} = \frac{\lambda e^{-b}}{\lambda e^{-b} + \gamma}\frac{g''(1)}{g'(1)}. \tag{31}$$

In a similar way, we consider the awareness breaking infectious edges. The R_0 shows the same value. The results are the same as that in Li et al. (2020). That means, we can get the following conclusions, first of all, two types of awareness reducing effects produce the same basic reproduction number. Second, the basic reproduction number has nothing to do with the risk perception coefficient α, but is related to the initial awareness coefficient b, and R_0 decreases with the increase of the initial awareness coefficient b. Third, when the initial awareness coefficient is zero, the value of R_0 is equal to the value in Miller-Volz (Volz, 2008; Miller, 2011) model.

3.2. Epidemic peak and final size

Here we will study the influence of infection risk perception on the final epidemic size and peak size of the disease in the scale-free network and Poisson network. The final epidemic size is $Z = 1 - S(\infty) = 1 - g(\theta(\infty))$. We consider the risk perception coefficient α and the speed of information transmission v. Among them, the α is reflected in $e^{-\alpha\rho}$, the v is reflected in equation (11).

We consider the dynamic procedure on the scale-free network and Poisson network. We change the risk perception coefficient α, the infection rate λ, and the speed of information transmission v, and then draw the dynamic curves by numerical simulation to study the effect of these parameters.

In Figs. 2–5, we consider the scale-free network. The ordinate is peak or final epidemic size which are the function of the speed of information transmission v. The blue curves correspond to using risk perception ρ as disease awareness, while the red curves correspond to using the prevalence I as disease awareness. As for ρ as awareness, we use models (22)–(27) and (11). As for I as awareness, we use models (16)–(21) and (11). We can get some conclusions. Firstly, we find that increasing the speed of information transmission v can decrease the peak and final size of disease with ρ as awareness, but does not change the peak and final size of disease with real disease I as awareness. Then as the speed of information transmission v increases, the peak and final size of the disease generated by ρ as awareness are getting closer and closer to the peak and final size of I as awareness. In addition, fixing risk perception coefficient α, an increasing in the infection rate λ can increase the peak and final size of the disease. Third, when we fix the infection rate λ, as the risk perception coefficient α increasing, both the peak and final size of the disease become smaller.

We also consider the Poisson network, the conclusions of awareness effect on peak size are the same as scale-free network. So, here, we don't put the numerical simulation results of awareness effects peak size on Poisson network. As for awareness effects final size, there are some differences from the scale-free network. Still, the final size increases with the rise of infection rate λ; the final size decreases with the rise of risk perception coefficients α. Still, as the speed of information transmission v

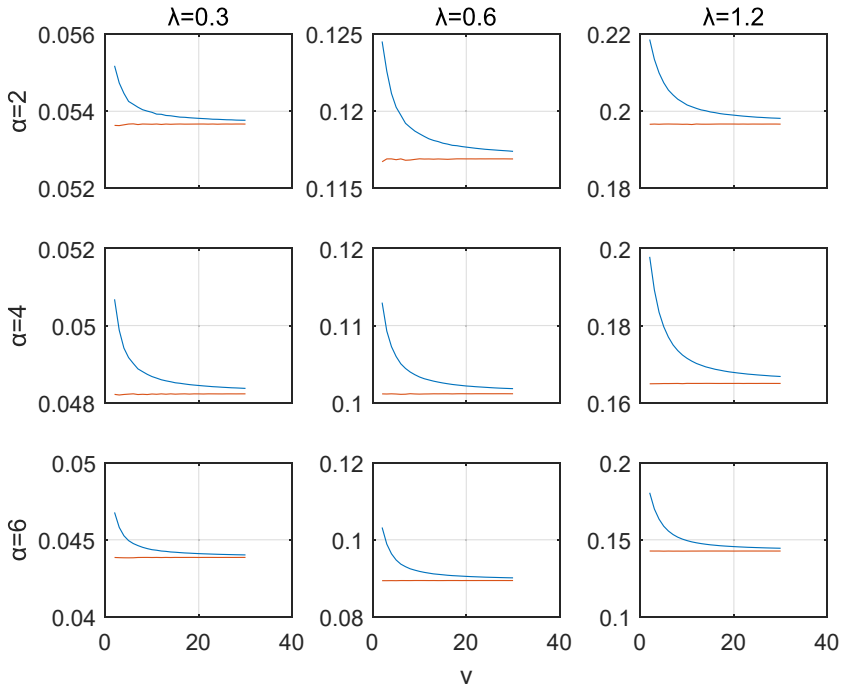

Fig. 2. The peak as a function of the speed v of information spread on a scale-free network with a degree distribution $p_k \propto k^{-2}$ for $k = 1, 2, \cdots, 60$, when awareness reduces the infection rate. The blue curves correspond to using risk perception $\rho(t)$ as disease awareness, while the red curves correspond to using the prevalence $I(t)$ as disease awareness. We consider three infection rates $\lambda = 0.3, 0.6, 1.2$. The recovery rate $\gamma = 1$. We consider three risk perception coefficients $\alpha = 2,4,6$. The speed of information transmission v varies from 2 to 30. The initial awareness coefficient b $= 0$. The initial conditions are $\theta_0 = 1$, $\varphi_0 = I_0 = \rho(0) = 0.01$.

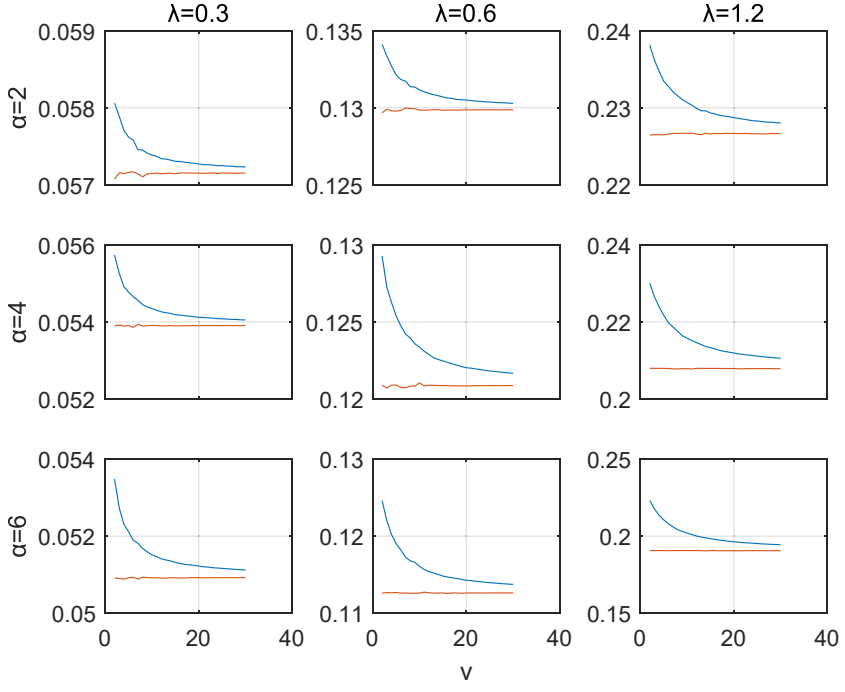

Fig. 3. The peak as a function of the speed v of information spread on a scale-free network when disease awareness breaks the infectious edges. The blue curves correspond to using risk perception $\rho(t)$ as disease awareness, while the red curves correspond to using the prevalence $I(t)$ as disease awareness. The network, disease parameters and initial conditions are the same as in Fig. 2.

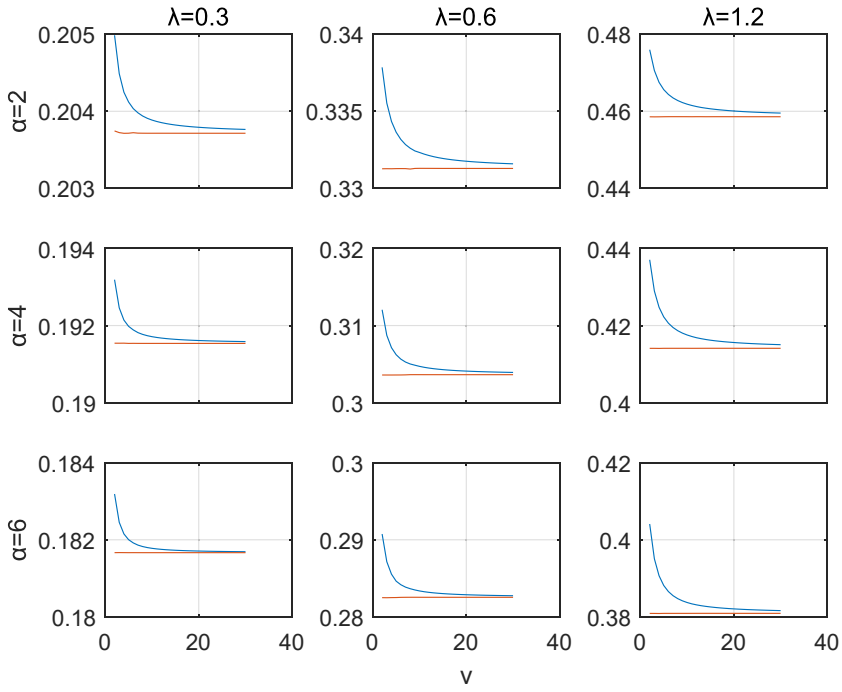

Fig. 4. The final size as a function of the speed v of information spread on a scale-free network when disease awareness reduces the infection rate. The blue curves correspond to using risk perception $\rho(t)$ as disease awareness, while the red curves correspond to using the prevalence $I(t)$ as disease awareness. The network, disease parameters and initial conditions are the same as in Fig. 2.

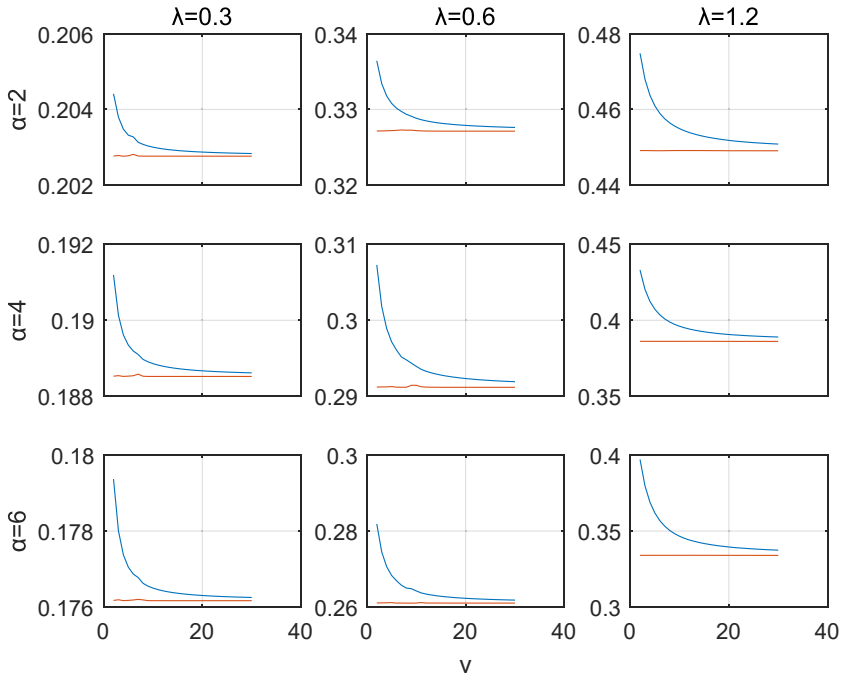

Fig. 5. The final size as a function of the speed v of information spread on a scale-free network when disease awareness breaks the infectious edges. The blue curves correspond to using risk perception $\rho(t)$ as disease awareness, while the red curves correspond to using the prevalence $I(t)$ as disease awareness. The network, disease parameters and initial conditions are the same as in Fig. 2.

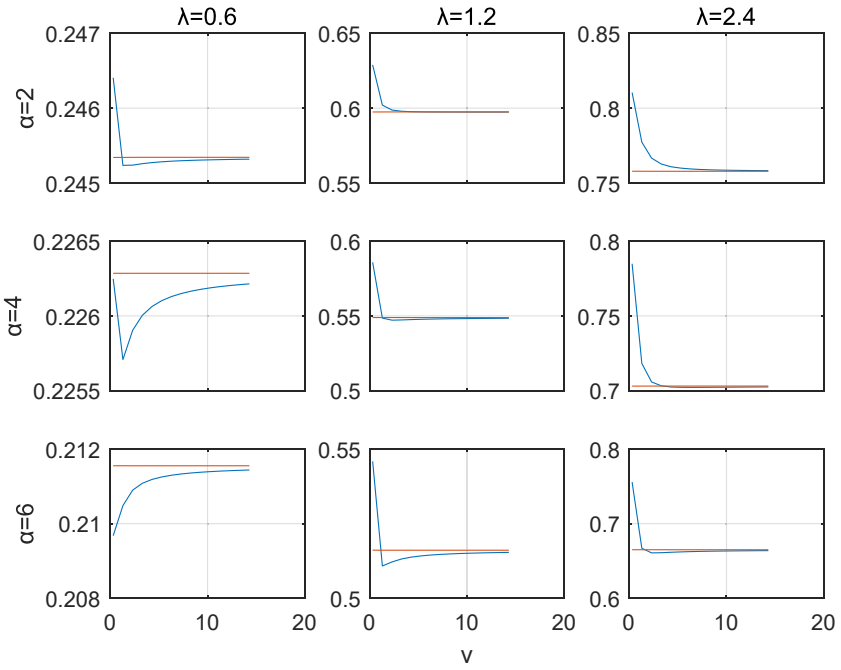

Fig. 6. The final size as a function of the speed v of information spread on a Poisson network with a degree distribution $\frac{3^k}{k!}e^{-3}$, when disease awareness reduces the infection rate. The blue curves correspond to using risk perception $\rho(t)$ as disease awareness, while the red curves correspond to using the prevalence $I(t)$ as disease awareness. We consider three infection rates $\lambda = 0.6, 1.2, 2.4$. The recovery rate $\gamma = 1$. We consider three risk perception coefficients $\alpha = 2,4,6$. The speed of information transmission v varies from 0.3 to 15. The initial awareness coefficient $b = 0$. The initial conditions are $\theta_0 = 1$, $\varphi_0 = I_0 = \rho(0) = 0.01$.

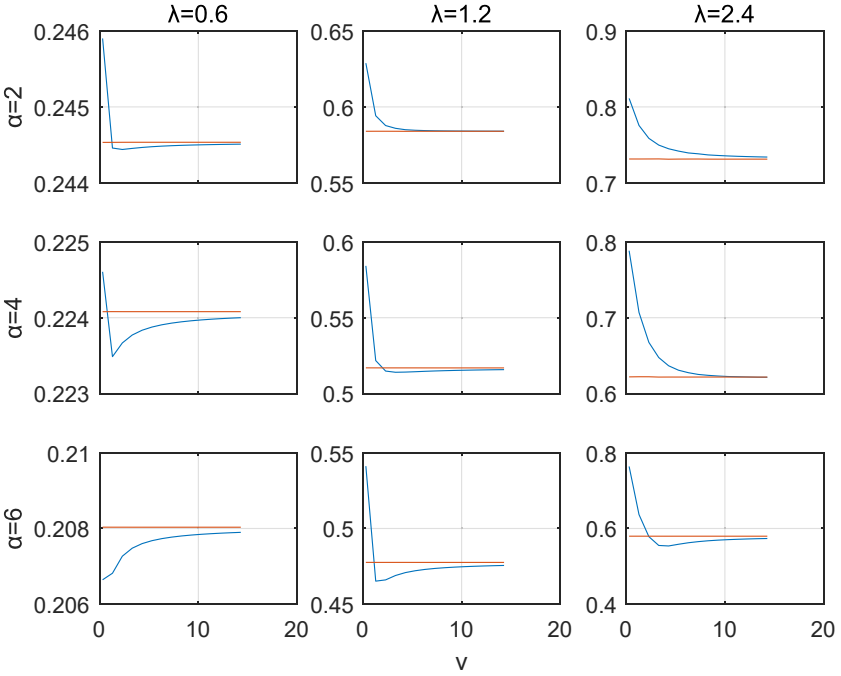

Fig. 7. The final size as a function of the speed v of information spread on a Poisson network when disease awareness breaks the infectious edges. The blue curves correspond to using risk perception $\rho(t)$ as disease awareness, while the red curves correspond to using the prevalence $I(t)$ as disease awareness. The network, disease parameters and initial conditions are the same as in Fig. 6.

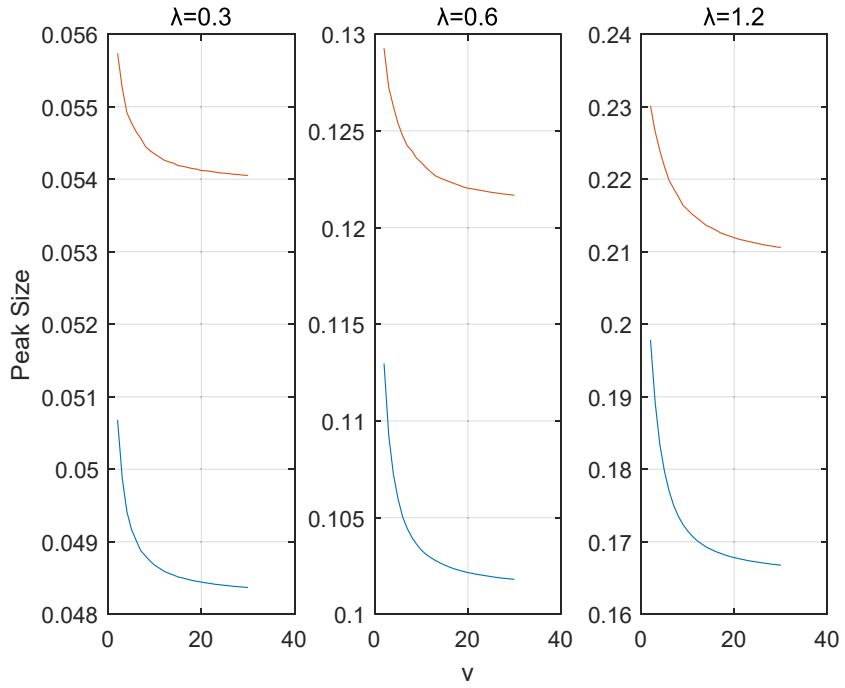

Fig. 8. The peak size as a function of the speed v of information spread on a scale-free network with $p_k \propto k^{-2}$ for $k = 1, 2, \cdots, 60$. The blue curves correspond to awareness reduces the infection rate, while the red curves correspond to awareness breaks the infectious edges. We consider three infection rates $\lambda = 0.3, 0.6, 1.2$. The recovery rate is $\gamma = 1$. The risk perception coefficient α is 4. The speed of information transmission v varies from 2 to 30. The initial awareness coefficient $b = 0$. The initial conditions are $\theta_0 = 1$, $\varphi_0 = I_0 = \rho(0) = 0.01$.

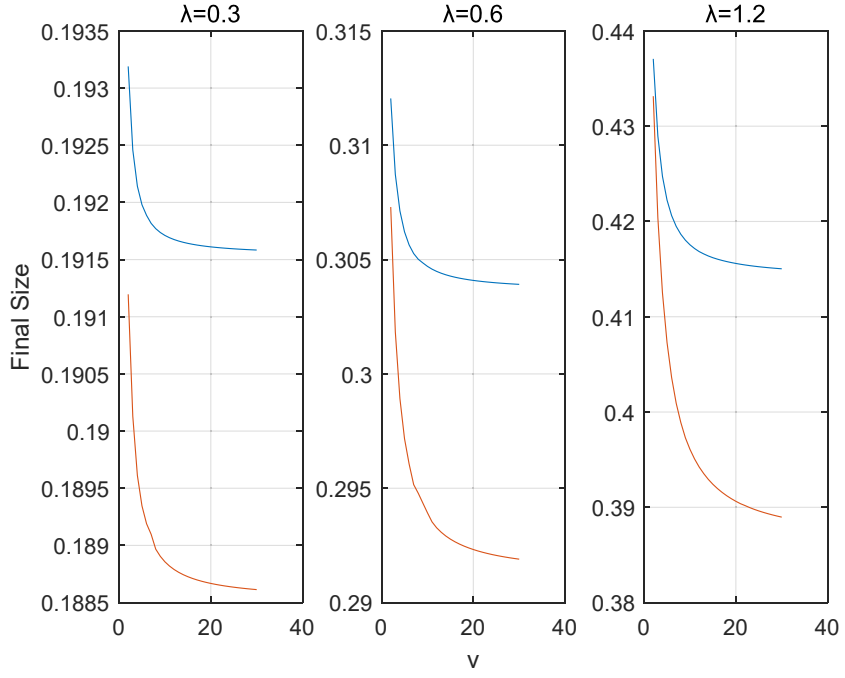

Fig. 9. The final size as a function of the speed v of information spread on a scale-free network. The blue curves correspond to awareness reduces the infection rate, while the red curves correspond to awareness breaks the infectious edges. The network, disease parameters and initial conditions are the same as in Fig. 8.

increases, the final size of the disease generated by the I as awareness don't change, but, as the speed of information transmission v increases, the final size of the disease generated by ρ as awareness maybe continue to decrease until it approaches the final size of I as awareness, or maybe decrease lower below the final size of I as awareness, then gradually increase and do not exceed it, the specific case depends on the choice of parameters. The results are presented in Figs. 6 and 7, also, there are two types of curves, the blue curves correspond to using risk perception ρ as disease awareness, while the red curves correspond to using the prevalence I as disease awareness.

In addition to that, we juxtaposed the two awareness reducing effects: awareness reduces infection rate and awareness breaks infectious edges, we compared the effects on the peak and final size. The result figures are showed in Figs. 8 and 9.

From Figs. 8 and 9, which consider the scale-free network, we can conclude that for reducing the final size, the effect of breaking contact network infectious edges is larger, for reducing the peak size, the effect of reducing the infection rate is larger. We have verified that the same conclusions are also true for Poisson networks. The figures for Poisson networks are not shown here.

4. Conclusion

We model the interaction of disease dynamics and risk perception on a two-layer random network that combines a social network layer with a contact network layer. We assume that individuals update their perception of infection risk via two means by communicate with their neighbors on the social network, including surveying their social network neighbors about the fraction of infected neighbors, and averaging their neighbors' perception of the risk. We found that, if information spreads much faster than disease, then all individuals converge on the true prevalence of the disease. On the other hand, if the two dynamics have comparable speed, the disease perception still converges to a value uniformly on the network, but the perception lags behind the true prevalence, and has a lower peak value.

To couple the disease and perception dynamics, we follow the idea in Li et al. (2020) to model the disease dynamics using the Miller-Volz model (Volz, 2008; Miller, 2011) on the contact network, and study the behavior change caused by the perception of infection risk. This behavior change may affect the disease dynamics either by reducing the transmission rate along the edges of the contact network, or by breaking edges and isolating the infectious individuals. Either effect is assumed to be influenced by the risk perception.

Our model uses the risk perception as disease awareness. Comparing to the results of Li et al. (2020) and similar models that use the disease prevalence as disease awareness, when the disease and information spreads have comparable speed, the lag of the risk perception in our model has complex influence on disease dynamics. On a scale-free network, both the peak size and the final size in our model are slightly larger than the results of the other models, implying that the lag slightly reduces the effect of behavior change caused by disease awareness. The difference is more pronounced when the information spread is slower. On a Poisson network, this is still true for peak size. This is because the lag in the disease perception results in less behavior change, and thus results in a higher peak.

On a Poisson network, the final size is also larger when the information spread is slow. However, as information spread speeds up, the final size of our model may become smaller than that of Li et al. (2020). This is because, for some intermediate information spread speed v, the higher peak in our model results in a perceived risk that is eventually larger than the prevalence when the prevalence passed its peak and declines. This causes a much stronger behavior change in our model that causes the prevalence to decrease faster than in the Li et al. (2020) model.

For both networks, as the speed of information spread increases towards infinity, the risk perception approaches the disease prevalence, and our results approaches the results of Li et al. (2020).

As Li et al. (2020), we consider two effects of disease awareness on disease dynamics: reducing the transmission rate along a random edge on the contact network, or breaking the edges of infectious nodes on the contact network.

We find that these two effects gives the same basic production number. This is because the basic reproduction number considers the disease dynamics near the disease-free equilibrium, when the prevalence is very small and the effect of disease awareness is negligible. Edge-breaking has a larger effect on reducing the final size, while reducing the transmission rate has a larger effect on reducing the peak size. This is true for both scale-free networks and Poisson networks.

For simplicity, our study does not consider the degree correlation between the contact network and the social network, even though our model can incorporate the correlation. Such correlation may have a significant effect on our results, and its effect is an interesting future research direction.

Declaration of competing interest

The authors declare that they have no known competing financial interests or personal relationships that could have appeared to influence the work reported in this paper.

Acknowledgments

This research was supported by National Natural Science Foundation of China (No.12271088) (ML), Natural Science Foundation of Shanghai (No. 21ZR1401000) (ML) and a discovery grant of Natural Sciences and Engineering Research Council Canada (JM), and two NSERC EIDM grants (OMNI and MfPH) (JM).

References

Akwara, P. A., Madise, N. J., & Hinde, A. (2003). Perception of risk of HIV/AIDS and sexual behaviour in Kenya. *Journal of Biosocial Science, 35*(3), 385–411.

Bagnoli, F., Lio, P., & Sguanci, L. (2007). Risk perception in epidemic modeling. *Physical Review E, 76*(6), Article 061904.

Ball, F., Sirl, D., & Trapman, P. (2010). Analysis of a stochastic SIR epidemic on a random network incorporating household structure. *Mathematical Biosciences, 224*(2), 53–73.

Chew, C., & Eysenbach, G. (2010). Pandemics in the age of twitter: Content analysis of tweets during the 2009 H1N1 outbreak. *PLoS One, 5*(11), Article e14118.

Dreessche, P., & Watmough, J. (2002). Reproduction numbers and sub-threshold endemic equilibria for compartmental models of disease transmission. *Mathematical Biosciences, 180*(1–2), 29–48.

Ferguson, N. (2007). Capturing human behaviour. *Nature, 446*(7137), 733.

Funk, S., Gilad, E., Watkins, C., & Jansen, V. A. (2009). The spread of awareness and its impact on epidemic outbreaks. *Proceedings of the National Academy of Sciences, 106*(16), 6872–6877.

Gallos, L. K., Song, C., & Makse, H. A. (2008). Scaling of degree correlations and its influence on diffusion in scale-free networks. *Physical Review Letters, 100*(24), Article 248701.

Ginsberg, J., Mohebbi, M. H., Patel, R. S., Brammer, L., & Brilliant, L. (2008). Detecting influenza epidemics using search engine query data. *Nature, 457*(7232), 1012–1014.

Gomez, S., Albert, D. G., Jesus, G. G., Conrad, P. V., Moreno, Y., & Arenas, A. (2013). Diffusion dynamics on multiplex networks. *Physical Review Letters, 110*(2), Article 028701.

Granell, C., Gómez, S., & Arenas, A. (2013). Dynamical interplay between awareness and epidemic spreading in multiplex networks. *Physical Review Letters, 111*, Article 128701.

Han, S., Zhuang, F., He, Q., Shi, Z., & Ao, X. (2014). Energy model for rumor propagation on social networks. *Physica A: Statistical Mechanics and Its Applications, 394*, 99–109.

Howard, L. (2006). *South African perceptions of risk and the social representations of HIV/AIDS*. Johannesburg, South Africa: University of the Witwatersrand, School of Human & Community Development. Psychology Masters Research Thesis.

Li, M., Wang, M., Xue, S., & Ma, J. (2020). The influence of awareness on epidemic spreading on random networks. *Journal of Theoretical Biology, 486*, Article 110090.

Magnan, R. E., Gibson, L. P., & Bryan, A. D. (2021). Cognitive and affective risk beliefs and their association with protective health behavior in response to the novel health threat of COVID-19. *Journal of Behavioral Medicine, 44*, 285–295.

Massaro, E., & Bagnoli, F. (2014). Epidemic spreading and risk perception in multiplex networks: A self-organized percolation method. *Physical Review E, 90*(5), Article 052817.

Miller, J. C. (2011). A note on a paper by Erik Volz: SIR dynamics in random networks. *Journal of Mathematical Biology, 62*(3), 349–358.

Peng, X., Li, C., Qi, H., Sun, G., Wang, Z., & Wu, Y. (2022). Competition between awareness and epidemic spreading in homogeneous networks with demography. *Applied Mathematics and Computation, 420*, Article 126875.

Riva, M. A., Benedetti, M., & Cesana, G. (2014). Pandemic fear and literature: Observations from Jack London's the scarlet plague. *Emerging Infectious Diseases, 20*(10), 1753–1757.

Rizzo, A., Frasca, M., & Porfiri, M. (2014). Effect of individual behavior on epidemic spreading in activity-driven networks. *Physical Review E, 90*(4), Article 042801.

Savadori, L., & Lauriola, M. (2022). Risk perceptions and COVID-19 protective behaviors: A two-wave longitudinal study of epidemic and post-epidemic periods. *Social Science & Medicine, 301*, Article 114949.

Stieglitz, S., & Linh, D. X. (2013). Emotions and information diffusion in social media—sentiment of microblogs and sharing behavior. *Journal of Management Information Systems, 29*(4), 217–248.

Volz, E. (2008). SIR dynamics in random networks with heterogeneous connectivity. *Journal of Mathematical Biology, 56*, 293–310.

Wang, C., Fu, S., Bai, X., & Bai, L. (2009). Risk perception in modeling malware propagation in networks. In *2009 WRI world congress on computer science and information engineering* (Vol. 3, pp. 35–39).

Wang, C., Yang, X., Xu, K., & Ma, J. (2014). SEIR-based model for the information spreading over SNS. *Acta Electronica Sinica, 42*(11), 2325.

Xiao, Y., Zhang, L., Li, Q., & Liu, L. (2019). MM-SIS: Model for multiple information spreading in multiplex network. *Physica A: Statistical Mechanics and Its Applications, 513*, 135–146.

Zhang, D. Z., & Padrino, J. C. (2017). Diffusion in random networks. *International Journal of Multiphase Flow, 92*, 70–81.

Zhang, M., Qin, S., & Zhu, X. (2021). Information diffusion under public crisis in BA scale-free network based on SEIR model—taking COVID-19 as an example. *Physica A: Statistical Mechanics and Its Applications, 571*, Article 125848.

Zhao, L., Wang, J., Chen, Y., Wang, Q., Cheng, J., & Cui, H. (2012). SIHR rumor spreading model in social networks. *Physica A: Statistical Mechanics and Its Applications, 391*(7), 2444–2453.